Supporting Information

for

Reaction of copper(II)-nitrosyl complex with hydrogen peroxide: putative formation of copper(I)-peroxynitrite intermediate

Biplab Mondal,*Apurba Kalita, Pankaj Kumar

Experimental Section

General:

All reagents and solvents were purchased from commercial sources and were of reagent grade. Acetonitrile was distilled from calcium hydride. Deoxygenation of the solvent and solutions were effected by repeated vacuum/purge cycles or bubbling with nitrogen for 30 minutes. NO gas was purified by passing through KOH and P_2O_5 column. UV-visible spectra were recorded on a Perkin Elmer Lamda 25 UV-visible spectrophotometer. FT-IR spectra were taken on a Perkin Elmer spectrophotometer with samples prepared either as KBr pellets or for solutions, in NaCl cell of one cm path length. Solution electrical conductivity was checked using a Systronic 305 conductivity bridge. ^{1}H-NMR spectra were obtained with a 400 MHz Varian FT spectrometer. Chemical shifts (ppm) were referenced either with an internal standard (Me_4Si) for organic compounds or to the residual solvent peaks. The X-band Electron Paramagnetic Resonance (EPR) spectra of the complexes and of the reaction mixtures were recorded on a JES-FA200 ESR spectrometer. Elemental analyses were obtained from a Perkin Elmer Series II Analyzer. The magnetic moment of complexes are measured on a Cambridge Magnetic Balance.

Single crystals were obtained from the reaction mixture. The intensity data were collected using a Bruker SMART APEX-II CCD diffractometer, equipped with a fine focus 1.75 kW sealed tube MoKa radiation (l = 0.71073 Å) at 273(3) K, with increasing w (width of 0.3° per frame) at a scan speed of 3 s/frame. The SMART software was used for data acquisition. Data integration and reduction were undertaken with SAINT and XPREP software. Multi-scan empirical absorption corrections were applied to the data using the program SADABS. Structures were solved by direct methods using SHELXS-97 and refined with full-matrix least squares on F^2 using SHELXL-97. All non-hydrogen atoms were refined anisotropically. Structural illustrations have been drawn with ORTEP-3 for Windows.

Synthesis of ligand, L

The ligand **L** was synthesized from the reaction of 2-ethyl-4-methyl-imidazole with formaldehyde in methanol by following a method reported earlier.

Yield: 85%. Elemental analyses: Calcd. (%) for $C_{13}H_{20}N_4$: C, 67.21; H, 8.68; N, 24.12. Found (%): C, 67.19; H, 8.68; N, 24.02. FT-IR (in KBr): 2964, 2842, 1614, 1529, 1455, 1071 cm^{-1}; ^{1}H-NMR (400 MHz, $CDCl_3$): ŭ$_{ppm}$, 3.53(2H), 2.44(4H), 1.87(6H), 1.08(6H). ^{13}C-NMR (100 MHz, $CDCl_3$): ŭ$_{ppm}$, 149.17, 129.09, 127.15, 23.29, 22.55, 13.66, 10.64. Mass: $(m+H^+)/z$: Calcd. 233.16; Found, 233.17.

Synthesis of the precursor complex $[Cu(L)_2](ClO_4)_2$

The precursor complex, $[Cu(L)_2](ClO_4)_2$ was synthesized from the reaction of hexaaquacopper(II) perchlorate and **L** by following the reported procedure.

Yield: 80%. Elemental Analyses: Calcd. for $C_{26}H_{40}Cl_2CuN_8O_8$: C, 42.95; H, 5.55; N, 15.41. Found (%): C, 42.93; H, 5.56; N, 15.32. FT-IR: 2976, 1633, 1455, 1150, 1114, 625cm^{-1}; magnetic moment, 1.60 BM. ESI-Mass: 527.24.

Synthesis of complex 1, $[Cu(L)_2(NO)](ClO_4)_2$

Complex **1**, $[Cu(L)_2(NO)](ClO_4)_2$ was synthesized from the reaction of the precursor complex and nitric oxide gas by following the reported procedure.

Yield: 70%. Elemental Analyses: Calcd. for $C_{26}H_{40}Cl_2CuN_9O_9$: C, 41.25; H, 5.32; N, 16.65. Found (%): C, 41.29; H, 5.31; N, 16.73. FT-IR (in KBr): 2921, 1662, 1620, 1475, 1384, 1242, 1108, 625 cm^{-1}. ESI-Mass: 557.46.

Synthesis of complex 2

Complex **1** (1.514 g ; 2 mmol) was dissolved in 20 ml of degassed acetonitrile and the solution was cooled to -20 °C. To this cold solution, pre-cooled hydrogen peroxide (70% v/v; 4μl) was added and the solution turned colorless. It was then stirred at room temperature for 1h; layered with degassed benzene (20 ml) and kept in freezer. Colorless crystals of complex **2** was obtained from this solution after 2 days. Yield: 0.827 g (~70%). FT-IR (KBr pellet): 2976, 1630, 1535, 1384 cm^{-1}.

Synthesis of complex 3

Complex **1** (1.514 g; 2 mmol) was dissolved in 20 ml of degassed acetonitrile and the solution was cooled to -20 °C. To this cold solution, pre-cooled hydrogen peroxide (70% v/v; 4 μl) was added and the solution turned colorless. It was then opened to air and stirred at room temperature for 2h to ensure the complete conversion of copper(I) to copper(II). Then the volume of the solution was reduced to 10 ml and layered with benzene. The mixture was then kept in freezer for overnight which resulted in green crystalline complex **3**. Yield: 1.172 g (~85%). **3**. UV-visible (acetonitrile): λ_{max} (ε / M^{-1} cm^{-1}) 720 nm (108) and 391 nm (340). FT-IR (KBr pellet): 2982, 1630, 1466, 1384, 1089, 625 cm^{-1}. Molar conductance: 244 S cm^{-1} mol^{-1}. The observed magnetic moment, 1.64 BM. X-band EPR: g_{av}, 2.0992 in acetonitrile at room temperature.

Reaction of 2,4-ditertiarybutylphenol with colorless solution obtained from the reaction complex 1 with hydrogen peroxide at -20 °C

Complex **1** (1.514 g; 2 mmol) was dissolved in 20 ml of degassed acetonitrile and the solution was cooled to -20 °C. To this cold solution, pre-cooled hydrogen peroxide (70% v/v; 4μl) was added and the solution turned colorless. To this a precooled solution (2 ml) of 2,4-ditertiarybutylphenol (10 mmol) was added and stirred for ½ h at -20 °C. The reaction mixture was then warmed to room temperature and dried under reduce pressure. The solid mass was then subjected to column chromatography using silica gel column to obtain pure 2,4-ditertiarybutyl-6-nitrophenol. Yield: ~65%.

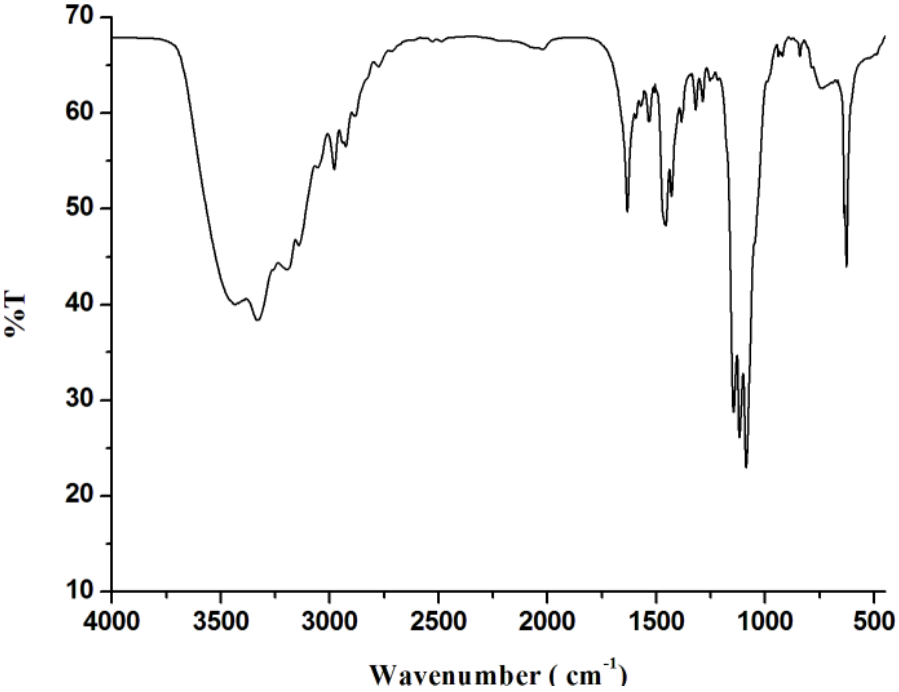

Figure S1: FT-IR spectrum of precursor complex in KBr.

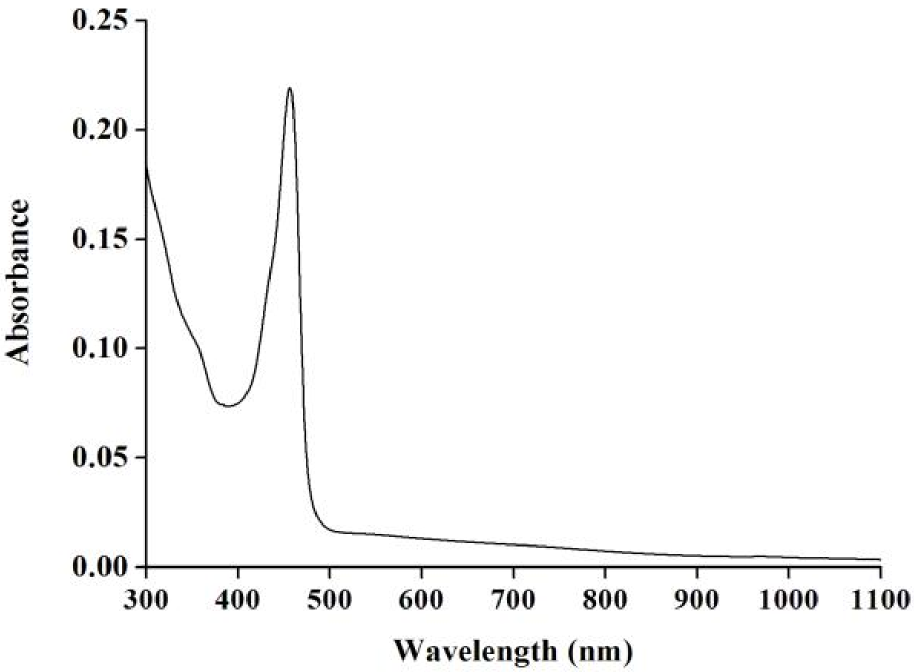

Figure S2: UV-visible spectrum of precursor complex in acetonitrile.

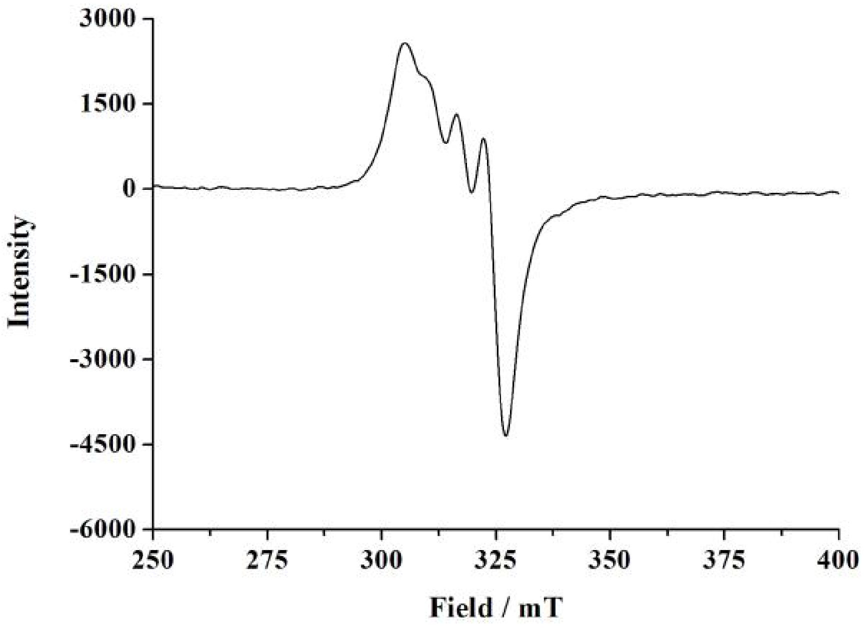

Figure S3: X-band EPR spectrum of precursor complex in acetonitrile at room temperature.

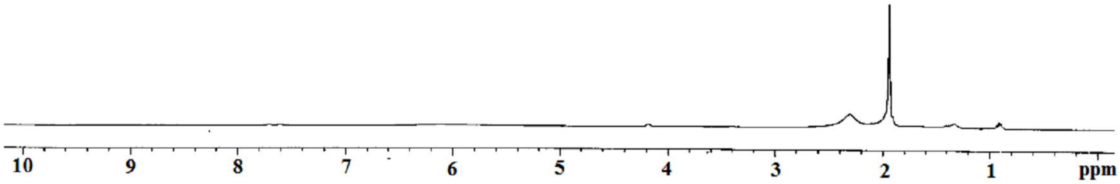

Figure S4: ^{1}H-NMR spectrum of precursor complex in CD_3CN.

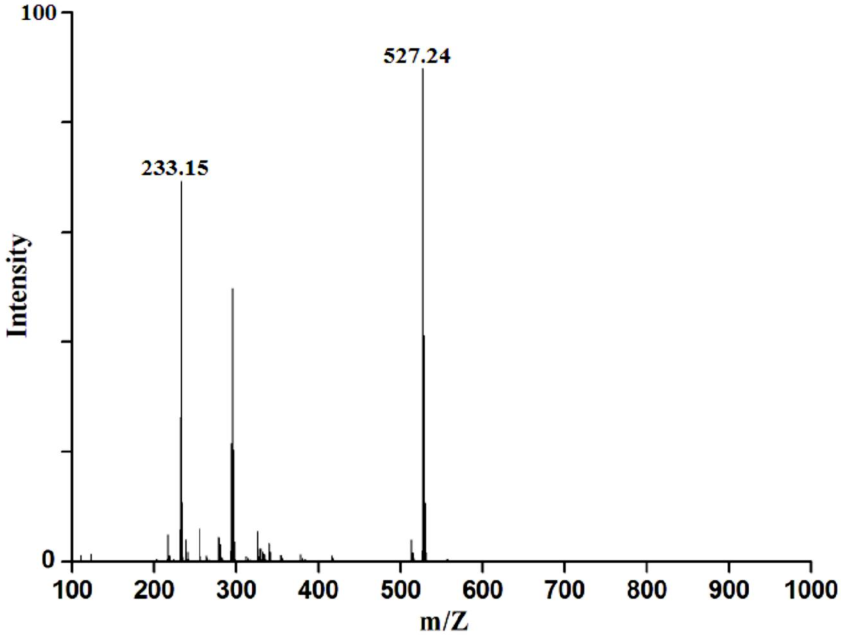

Figure S5: ESI-Mass spectrum of precursor complex in methanol.

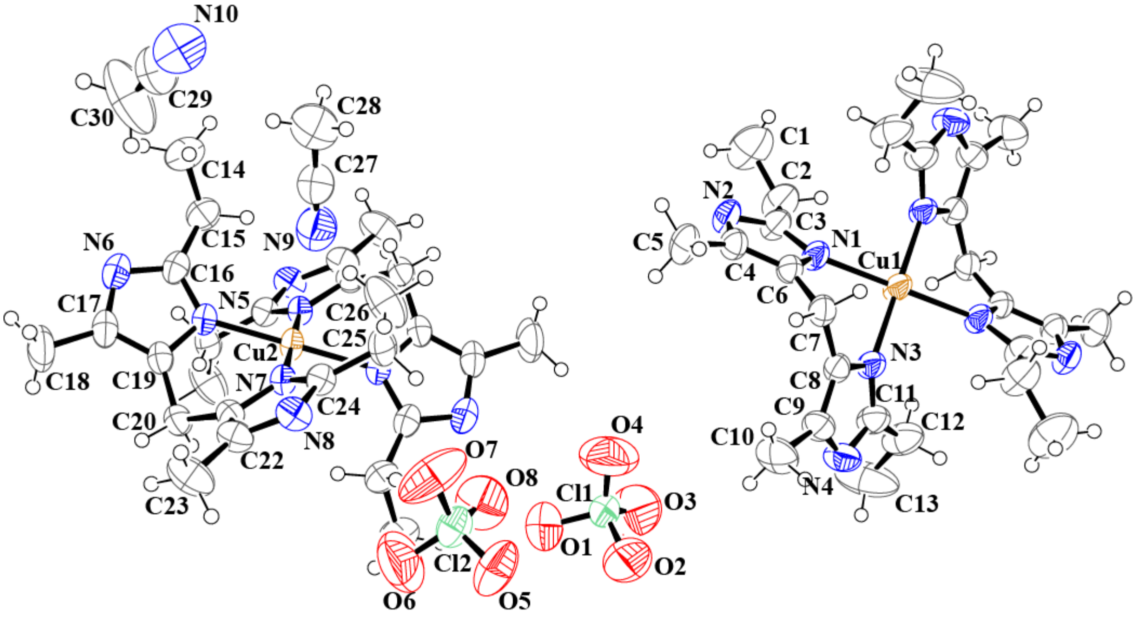

Figure S6: ORTEP diagram of precursor complex (50% thermal ellipsoid plot).

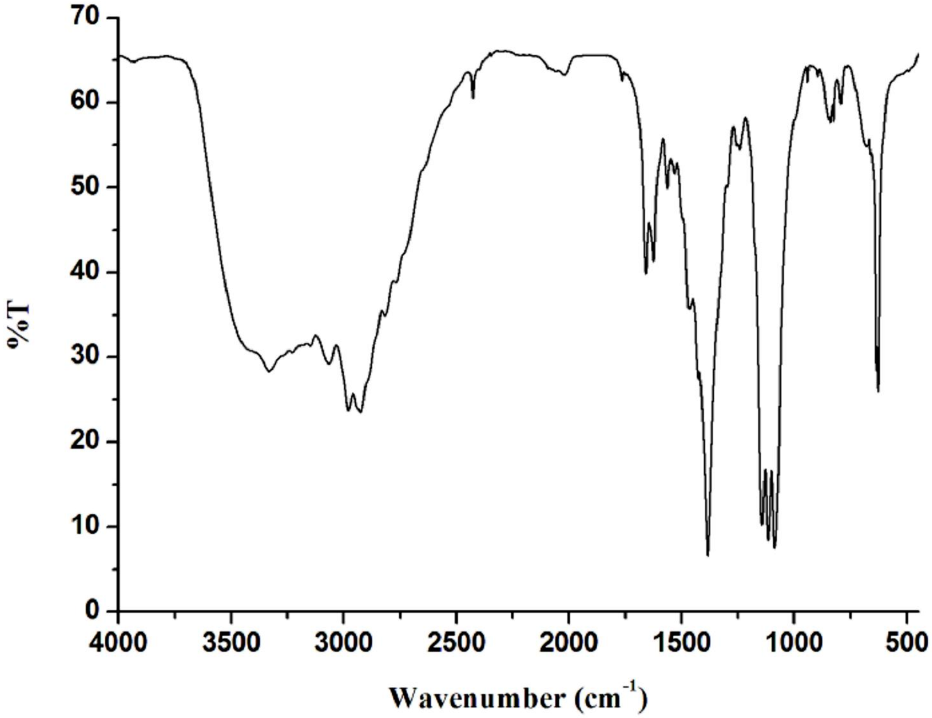

Figure S7: FT-IR spectrum of complex **1** in KBr.

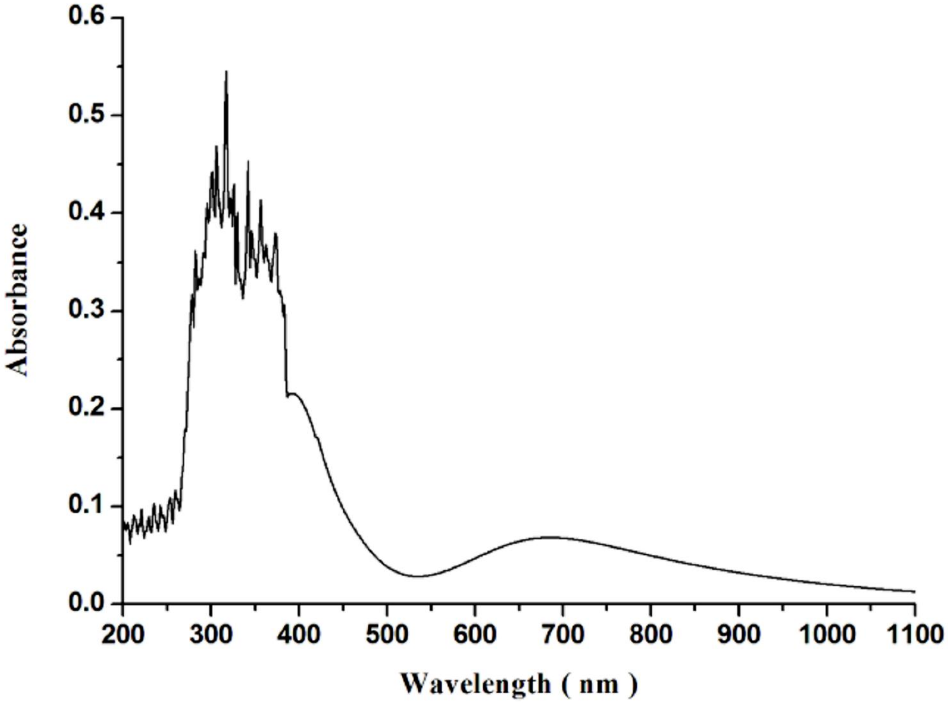

Figure S8: UV-visible spectrum of complex **1** in acetonitrile solvent at room temperature.

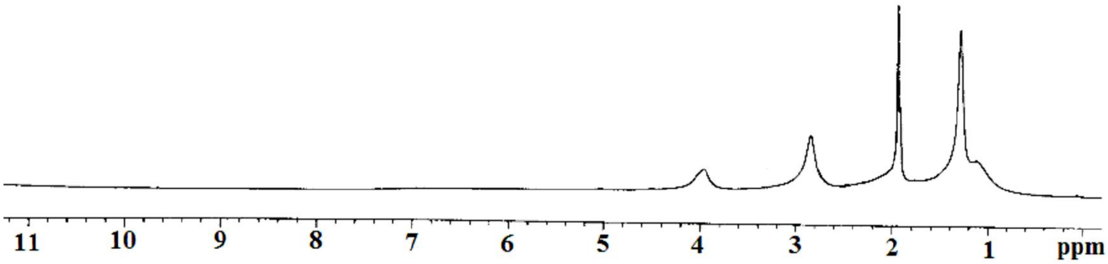

Figure S9: ^{1}H-NMR spectrum of complex **1** in CD_3CN (peak broadening is due to the presence of very less amount of Cu(II) impurities in solution).

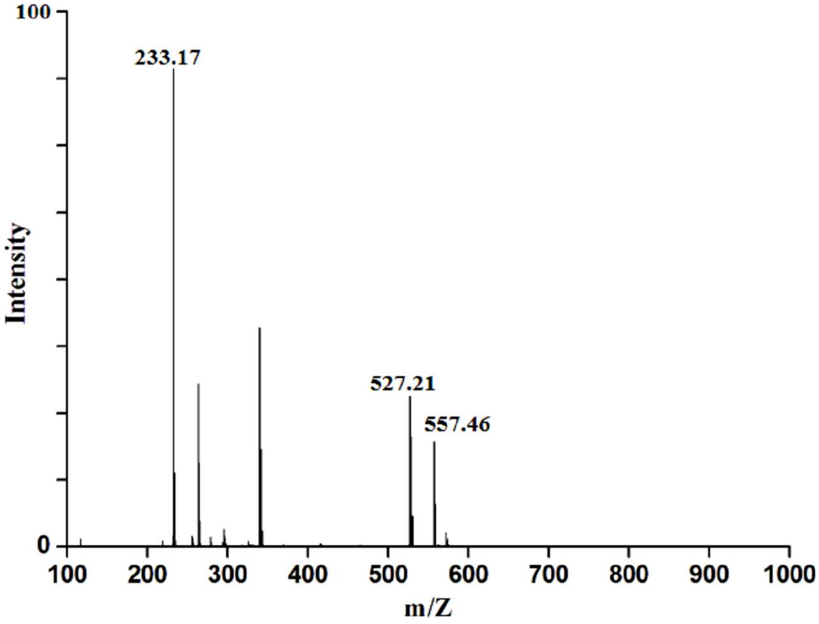

Figure S10: ESI-Mass spectrum of complex **1** in acetonitrile.

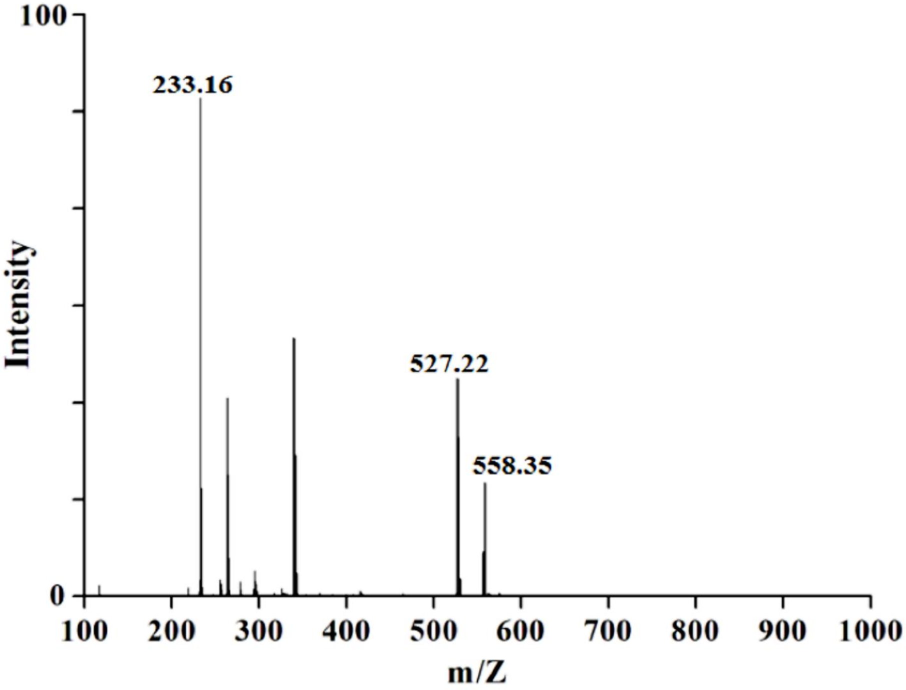

Figure S11: ESI-Mass spectrum of ^{15}NO labelled complex **1** in acetonitrile.

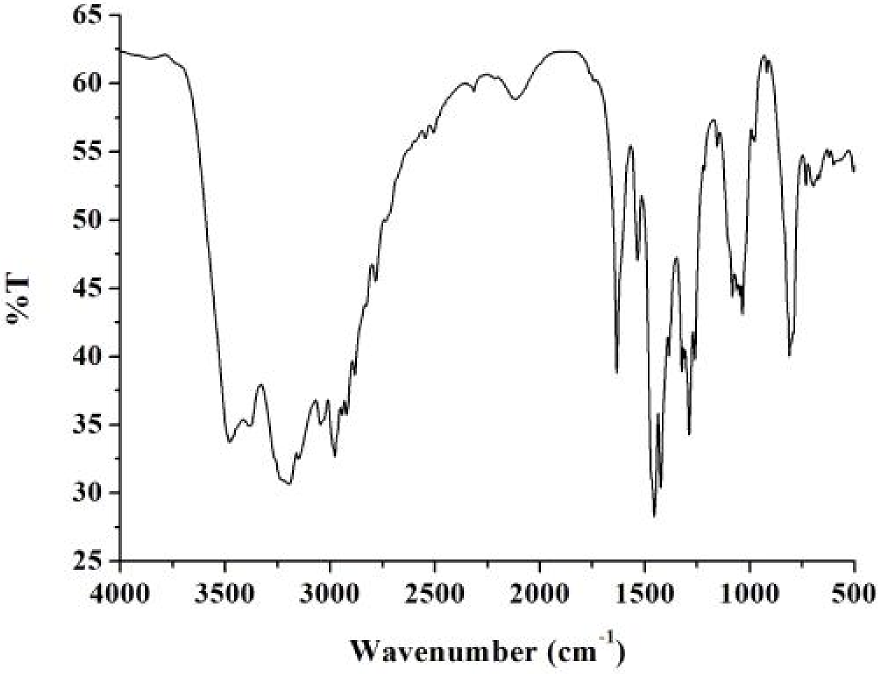

Figure S12: FT-IR spectrum of complex **2** in KBr.

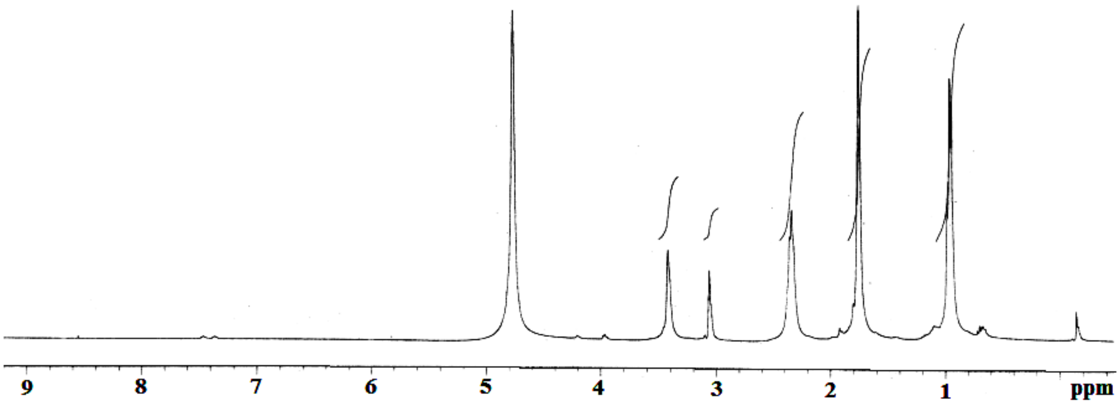

Figure S13: ^{1}H-NMR spectrum of complex **2** in methanol-d_4.

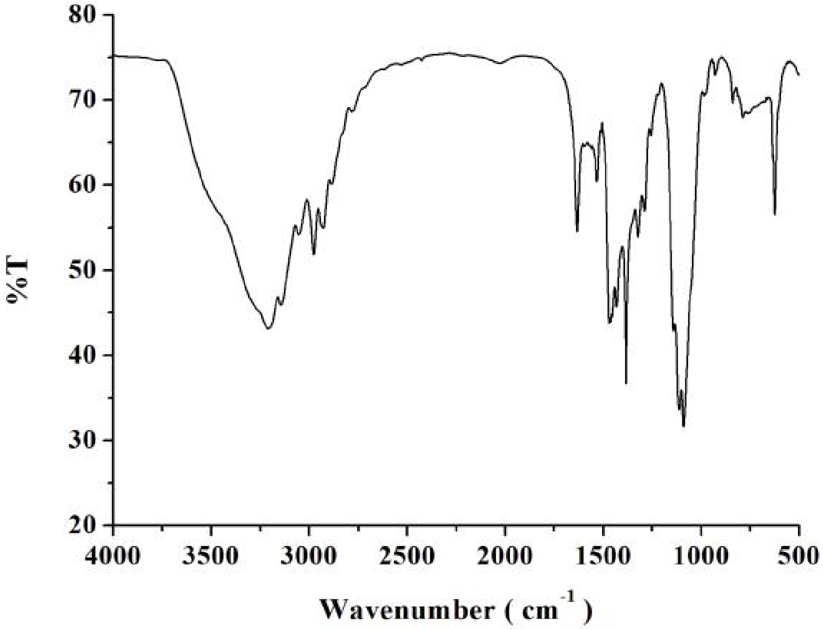

Figure S14: FT-IR spectrum of complex **3** in KBr.

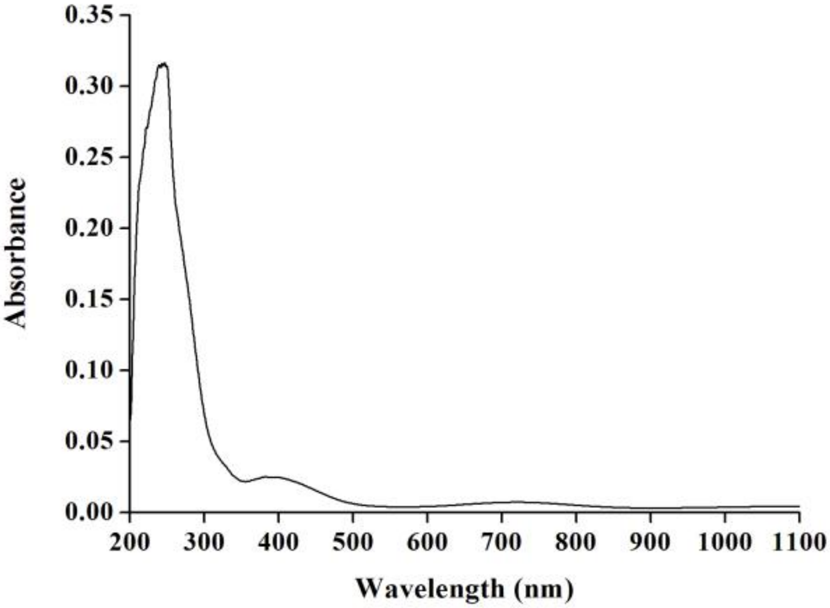

Figure S15: UV-visible spectrum of complex **3** in acetonitrile.

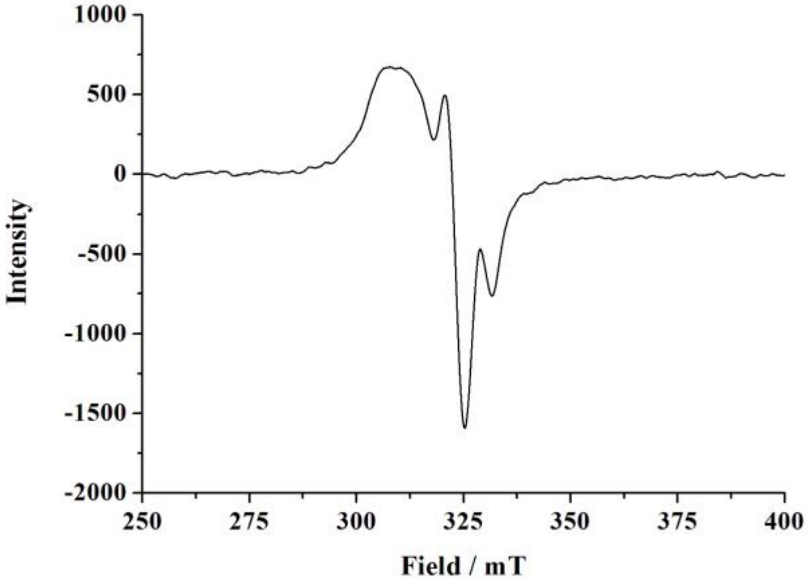

Figure S16: X-band EPR spectra of the complex **3** in acetonitrile solvent at room temperature.

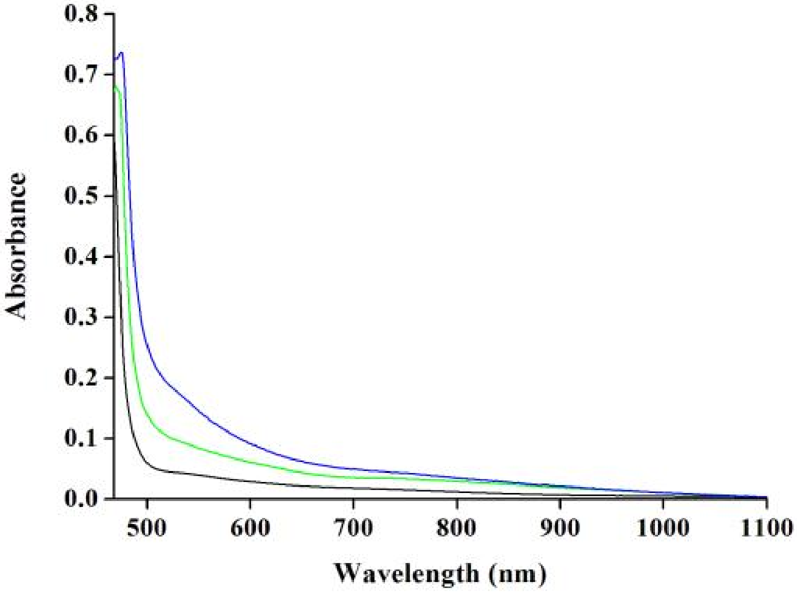

Figure S17: UV-visible spectra of precursor complex (black), after addition of one equivalent of KO_2 (blue) in acetonitrile. Green trace represents a spectrum at an intermediate time.

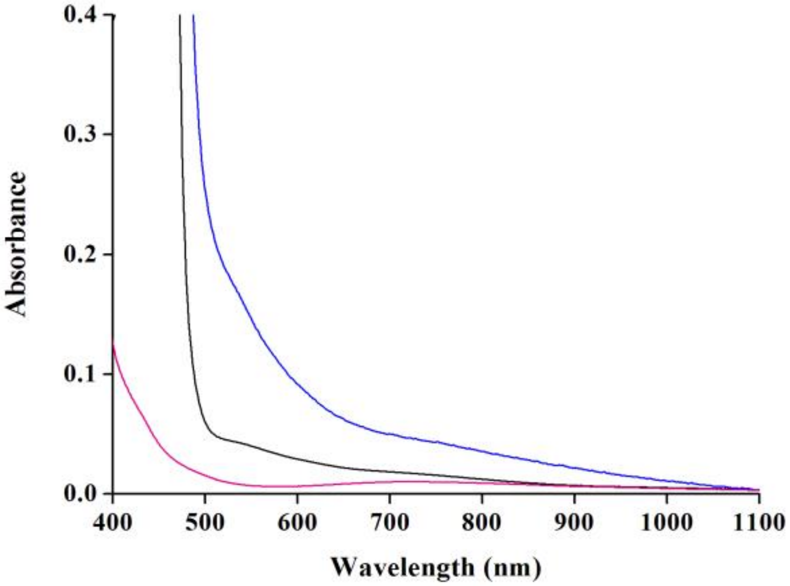

Figure S18: UV-visible spectra of precursor complex (black), after addition of one equivalent of KO_2(blue) and after addition of NO to the above mixture (pink) in acetonitrile.

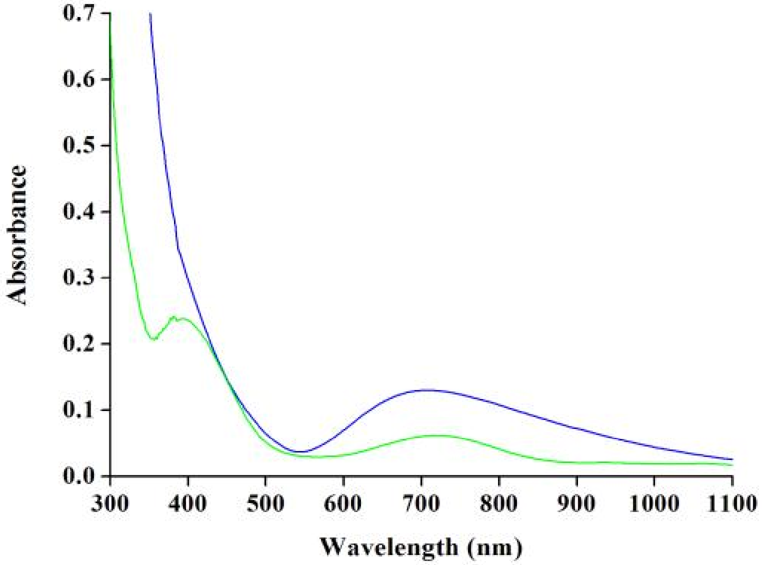

Figure S19: UV-visible spectra of complex **1** (blue) and after addition of one equivalent of KO_2 (green) in acetonitrile.

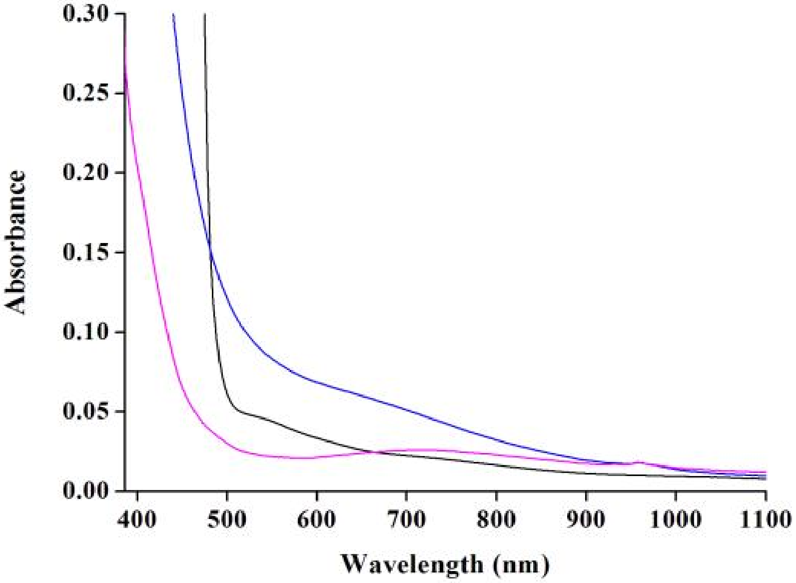

Figure S20: UV-visible spectra of precursor complex (black), after addition of one equivalent of H_2O_2 (blue) and after addition of NO to the above mixture (pink) in acetonitrile.

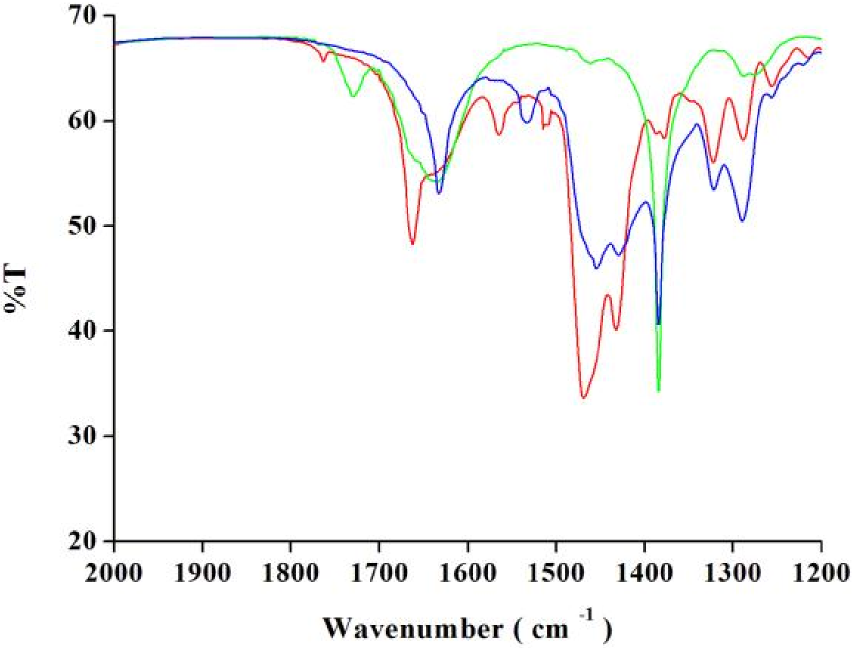

Figure S21: FT-IR spectra of complexes **1**(red), **2** (green), **3** (blue) in KBr.

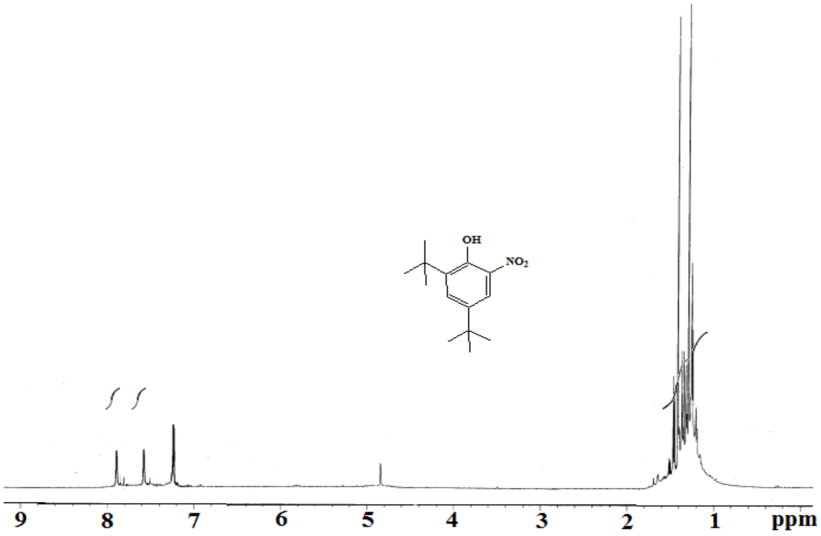

Figure S22: ^{1}H-NMR spectrum of 2, 4-di-tert-butyl-6-nitro-phenol in CD_3Cl.

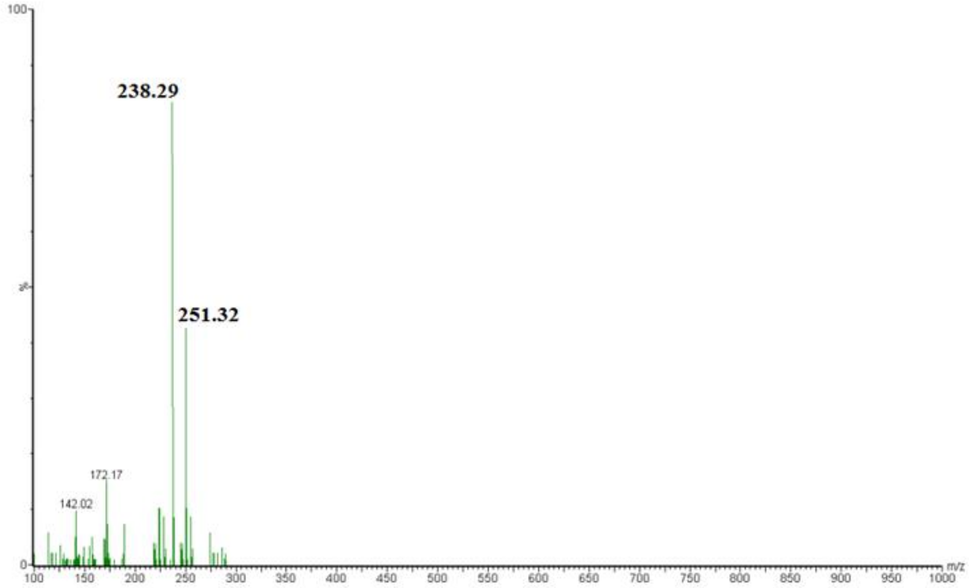

Figure S23: ESI-Mass spectrum of 2, 4-di-tert-butyl-6-nitro-phenol in methanol.

Table S1:

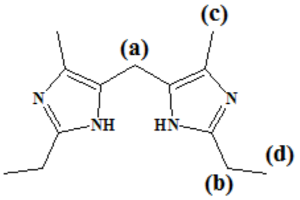

Chemical Shift (δ_{ppm})	Ligand (L)	Complex 1	Complex 2
(a)	3.53	3.96	3.42
(b)	2.59	2.84	3.06
(c)	1.87	1.91	2.33
(d)	1.08	1.28	0.96

Table S1. Crystallographic data for complexes **2** and **3.**

	Complex 2	Complex 3
Formulae	$C_{26} H_{36} Cu N_9 O_7$	$C_{26} H_{36} Cl Cu N_9 O_7$
Mol. wt.	650.19	685.64
Crystal system	Monoclinic	Monoclinic
Space group	P 2/c	P 21/c
Temperature /K	296(2)	293(2)
Wavelength /Å	0.71073	0.71073
a /Å	9.3665(10)	19.5792(16)
b /Å	9.6913(11)	9.3484(8)
c /Å	18.1622(18)	18.7219(16)
Ŭ/°	90.00	90.00
ɓ/°	90.203(5)	102.510(5)
Ả/°	90.00	90.00
V/ $Å^3$	1648.6(3)	3345.4(5)
Z	2	4
Density/Mgm^{-3}	1.310	1.361
Abs. Coeff. /mm^{-1}	0.716	0.787
Abs. correction	None	None
F(000)	680.0	1428
Total no. of reflections	7344	8345
Reflections, *I* > 2ů*(I)*	5057	3561

Max. 2ɗ/°	35.54	28.44
Ranges (h, k, l)	-14<= h <=15 -15<= k <=14 -29<= l <= 29	-26<= h <=23 -12<= k <=12 -25<= l <= 20
Complete to 2ɗ (%)	97.3	98.9
Refinement method	Full-matrix least-squares on F^2	Full-matrix least-squares on F^2
Goof (F^2)	1.071	1.055
R indices [*I* > 2ů*(I)*]	0.0664	0.0847
R indices (all data)	0.0838	0.1617

Table S2. Selected bond length (Å) for complexes **2** and **3.**

	Complex 2	Complex 3
Cu(1)-N(1)	2.122(2)	1.985(5)
Cu(1)-N(3)	1.984(2)	2.052(6)
Cu(1)-O(1)	2.386(3)	2.208(6)
Cu(1)-O(2)	-	2.637(8)
C(2)-C(1)	1.509(5)	1.49(1)
C(2)-C(3)	1.494(3)	1.49(1)
C(3)-N(1)	1.322(3)	1.332(8)
C(3)-N(2)	1.354(3)	1.333(8)
C(4)-N(2)	1.384(3)	1.386(9)
C(6)-N(1)	1.395(3)	1.401(8)
C(4)-C(5)	1.485(4)	1.47(1)
C(4)-C(6)	1.358(3)	1.35(1)
C(7)-C(6)	1.496(3)	1.494(9)
C(7)-C(8)	1.486(3)	1.49(1)
N(9)-O(1)	-	1.24(1)
C(9)-C(10)	1.497(3)	1.48(1)
C(11)-C(12)	1.490(3)	1.50(1)
C(12)-C(13)	1.504(4)	1.44(3)

Table S3. Selected bond angles (°) for complexes **2** and **3.**

	Complex2	Complex3
N(1)-Cu(1)-N(3)	90.24(7)	90.2(2)
Cu(1)-N(1)- C(3)	130.4(1)	130.7(4)
Cu(1)-N(1)- C(6)	120.0(1)	123.7(4)
Cu(1)-N(3)- C(8)	124.2(1)	123.3(5)

Cu(1)-N(3)-C(11)	129.3(1)	130.4(5)
N(1)-Cu(1)-O(1)	104.87(7)	87.5(2)
N(3)-Cu(1)-O(1)	84.71(7)	161.3(2)
C(1)-C(2)-C(3)	114.2(2)	115.3(7)
N(2)-C(3)-N(1)	110.0(2)	110.5(6)
C(3)-N(2)-C(4)	108.5(2)	109.0(6)
C(3)-N(1)-C(6)	106.7(2)	105.5(6)
C(5)- C(4)-C(6)	131.6(2)	133.2(7)
C(4)-C(6)-C(7)	130.3(2)	130.7(7)
C(6)-C(7)-C(8)	111.7(2)	114.2(6)
C(8)-C(9)-C(10)	132.5(2)	132.2(7)
C(8)-N(3)-C(11)	106.5(2)	105.9(6)
C(12)-C(11)-N(3)	127.4(2)	127.4(8)
C(11)-C(12)-C(13)	114.3(2)	115(1)